Hadal biosphere: Insight into the microbial ecosystem in the deepest ocean on Earth

Takuro Nunoura[a,1], Yoshihiro Takaki[a,b], Miho Hirai[a], Shigeru Shimamura[b], Akiko Makabe[c,d,2], Osamu Koide[a], Tohru Kikuchi[e], Junichi Miyazaki[b], Keisuke Koba[c], Naohiro Yoshida[d,3], Michinari Sunamura[f], and Ken Takai[b]

[b]Department of Subsurface Geobiological Analysis and Research and [a]Research and Development Center for Marine Biosciences, Japan Agency for Marine-Earth Science & Technology, Yokosuka 237-0061, Japan; [c]Institute of Agriculture, Tokyo University of Agriculture and Technology, Fuchu, Tokyo 183-8509, Japan; [d]Department of Environmental Science and Technology, Tokyo Institute of Technology, Midori-ku, Yokohama 226-8502, Japan; [e]Graduate School of Nanobioscience, Yokohama City University, Kanazawa-ku, Yokohama 236-0027, Japan; and [f]Department of Earth and Planetary Science, University of Tokyo, Bunkyo-ku, Tokyo 113-0033, Japan

Hadal oceans at water depths below 6,000 m are the least-explored aquatic biosphere. The Challenger Deep, located in the western equatorial Pacific, with a water depth of ~11 km, is the deepest ocean on Earth. Microbial communities associated with waters from the sea surface to the trench bottom (0 ~10,257 m) in the Challenger Deep were analyzed, and unprecedented trench microbial communities were identified in the hadal waters (6,000 ~10,257 m) that were distinct from the abyssal microbial communities. The potentially chemolithotrophic populations were less abundant in the hadal water than those in the upper abyssal waters. The emerging members of chemolithotrophic nitrifiers in the hadal water that likely adapt to the higher flux of electron donors were also different from those in the abyssal waters that adapt to the lower flux of electron donors. Species-level niche separation in most of the dominant taxa was also found between the hadal and abyssal microbial communities. Considering the geomorphology and the isolated hydrotopographical nature of the Mariana Trench, we hypothesized that the distinct hadal microbial ecosystem was driven by the endogenous recycling of organic matter in the hadal waters associated with the trench geomorphology.

hadal | trench | niche separation | nitrification | Challenger Deep

Microbial life in the dark ocean below mesopelagic water (corresponding to 200- to 1,000-m depth range) is thought to be primarily supported by the sinking organic carbon from surface waters. However, it has recently been revealed that the deep-sea biogeochemical cycles are more complex than previously expected and that the mismatch between the organic carbon supply and microbial heterotrophic demand has led to imbalances in some oceans (1–4). Currently, the contribution of chemolithoautotrophy and mixotrophy to the biogeochemical cycle (e.g., dark carbon fixation coupled with nitrification and sulfur oxidations) is also recognized as another significant organic carbon source in the dark ocean (3, 5, 6). It has been estimated that the dissolved inorganic carbon fixation in the dark ocean by these organisms could be on the same order-of-magnitude as heterotrophic biomass production (3, 5).

Hadal oceans at water depths below 6,000 m are comprised almost exclusively of trenches and are the least-explored aquatic biosphere on Earth. Trench environments are differentiated from upper abyssal oceans by their elevated hydrostatic pressure and their hydrotopographically isolated nature, whereas other physical and chemical conditions, such as temperature, salinity, dissolved oxygen, and nutrients are comparable to those in abyssal oceans (7–9). The microbiological and geochemical investigations of hadal waters have been limited (10), in contrast to the long history of hadal benthic microbiological studies occurring since the 1950s (11). To date, many piezophiles and piezotolerant bacteria have been isolated from hadal benthic habitats, and their phenotypical and genomic features have been characterized to be distinct from those of the close relatives obtained from shallow marine environments (12). As one of the major biogeochemical

traits, a significantly higher microbial carbon turnover rate has been identified in hadal sediments than that in adjacent abyssal plain sediments (13). Furthermore, Jamieson et al. indicated that the potential trench-specific distribution of eukaryotes is likely a result of the hydrostatic pressure and hydrotopographical isolation (7).

The Challenger Deep in the Mariana Trench is the deepest ocean on Earth, and its geology, current patterns, water chemistries, and benthic microbial communities have been relatively well studied (8, 9, 13–17). However, the hadal aquatic microbial communities in the Challenger Deep remain completely uncharacterized. This study aims to characterize the microbial community compositions and functions of the hadal water microbial ecosystem.

Results

Geochemical and Physical Environments. Water samples were taken in a total of three dives of the remotely operated vehicle (ROV) *ABISMO* at the same station (11–22.25′N, 142–42.75′E) on the Challenger Deep. The temperature and salinity profiles were

Significance

Although many microbial explorations for hadal sediments began in the 1950s, the hadal water is the least-explored microbial biosphere. In this study, unexpected microbial ecosystems associated with the hadal trench water were discovered down to a 10,257-m water depth in the Challenger Deep of the Mariana Trench, which is the deepest ocean on Earth. We found the enrichment of heterotrophic population in the hadal water (6,000 ~10,257 m) microbial communities, whereas the chemolithotrophic populations were more abundant in the upper abyssal waters. This observation suggested that the hadal microbial biosphere was supported by the endogenous recycling of organic matter in the hadal waters associated with the trench geomorphology.

similar to previous observations, and the salinity slightly increased at depths greater than 9,000 m below the surface (mbs) (8, 9, 18). The sea surface temperature was 29.1 °C; the potential temperature decreased to 1.02 °C at 10,257 mbs. The sea surface salinity was 34.2, and the maximum (34.8) and minimum (34.4) salinities were found at ~150 and 400 mbs, respectively (Fig. 1A). The salinity was constant at ~34.6 below 1,500 mbs and slightly increased below 9,000 mbs, as reported in previous studies (9, 18). The dissolved oxygen concentration (DO) at the sea surface was 219 μM and decreased to 62.5 μM at 500 mbs (Fig. 1B and Dataset S1). Then, the DO increased to 156 μM at 4,000 mbs and presented relatively constant concentrations between 156 μM and 172 μM below 4,000 mbs. The nitrate concentration at the sea surface was 0.22 μM, and it drastically increased along the thermo- and chemoclines (200–400 mbs) (Fig. 1B and Dataset S1). The maximum nitrate concentration (41.2 μM) was detected at 1,500 mbs, and constant nitrate concentrations (36.2–36.5 μM) were found below 5,000 mbs. The nitrite concentrations were less than 0.07 μM (detection limit <0.01 μM) throughout the water column. The ammonium concentrations were under the detection limit (detection limit <0.1 μM). The natural abundances of ^{15}N and ^{18}O of nitrate were 4.7–7.4‰ and 2.1–4.5‰, respectively (Fig. 1C and Dataset S1). The $\delta^{15}N$ and $\delta^{18}O$ values of deep nitrate were similar to previously reported data in other oceanic regions (19). The temperature and salinity profiles suggest the presence of at least five types of water masses throughout the depth profile: surface water (above 50 mbs), high salinity water (~150 mbs), low salinity water (~400 mbs), mesopelagic water (above 2,000 mbs), and deep water (below 2,000 mbs) (Fig. 1A). No significant change in the inorganic nutrients and isotopic signatures of nitrate between the hadal (below 6,000 mbs) and abyssal (below 4,000 m) waters was found, which was similar to a previous study (18) (Fig. 1B).

Cellular and Viral Abundance. The maximum cell abundance was found at 51 mbs (6.4×10^5 cells/mL) and the abundance decreased to a depth of 1,499 mbs (1.5×10^4 cells/mL) (Fig. 1D and Dataset S1). Below 2,000 mbs the cell abundance was relatively constant but gradually decreased with increasing depth, and the

cell abundance of the bottom waters was ~6×10^3 cells/mL. The abundance of virus-like particles (VLPs) increased from the sea surface to 101 mbs (5.8×10^6 particles/mL) and then decreased with increasing depth to 1,499 mbs (3.4×10^4 particles/mL). The VLP abundance increased at 2,000 mbs (2.4×10^5 particles/mL), and relatively constant VLP abundance was observed below 2,000 mbs ($2.2–3.6 \times 10^5$ particles/mL) (Fig. 1D). The maximum and minimum VLP-prokaryote ratio (VPR) was found at 147 and 1,499 mbs, respectively. The VPR below 2,000 mbs slightly increased with increasing depth; however, there were a few exceptions. The transition of microbial and viral abundance profiles between 1,500 and 2,000 mbs is likely equivalent to the water–mass interface.

SSU rRNA Gene Community Structures. Both tag sequencing and clone analyses were applied to investigate the prokaryotic small subunit (SSU) rRNA gene community structure along the water column on the Challenger Deep (Fig. 2 and Dataset S2). Overall, the niche separation at the species to phylum levels along the water column was identified. The tag sequence populations were grouped along the water column at the species level, as shown by the Jaccard and Bray–Curtis similarity matrixes: the euphotic zone (above 101 mbs), the mesopelagic to abyssopelagic waters (202–5,000 mbs), and the trench waters (below 6,001 mbs); a similar trend was also found at higher taxonomic levels (Fig. 3 and Figs. S1 and S2).

In the euphotic zone, obligately phototrophic *Prochlorococcus* and potentially photoheterotrophic bacterial lineages, such as SAR11 and *Bacteroidetes* (20, 21), dominated the prokaryotic SSU rRNA gene communities. The high abundance of *Actinobacteria* only occurred above 147 mbs, which implies the occurrence of phototrophic metabolism (22). SAR11 also dominated the SSU rRNA gene communities in aphotic waters above 2,000 mbs, and its abundance decreased drastically at 3,000 mbs. Below 147 mbs, thaumarchaeal phylotypes became the predominant populations; its relative abundance decreased with increasing trench water depth (Fig. 2). The abundance of SAR324, a potential chemolithoautotrophic deltaproteobacterial subgroup (6, 23, 24), also increased at 147 mbs and was detected as one of the
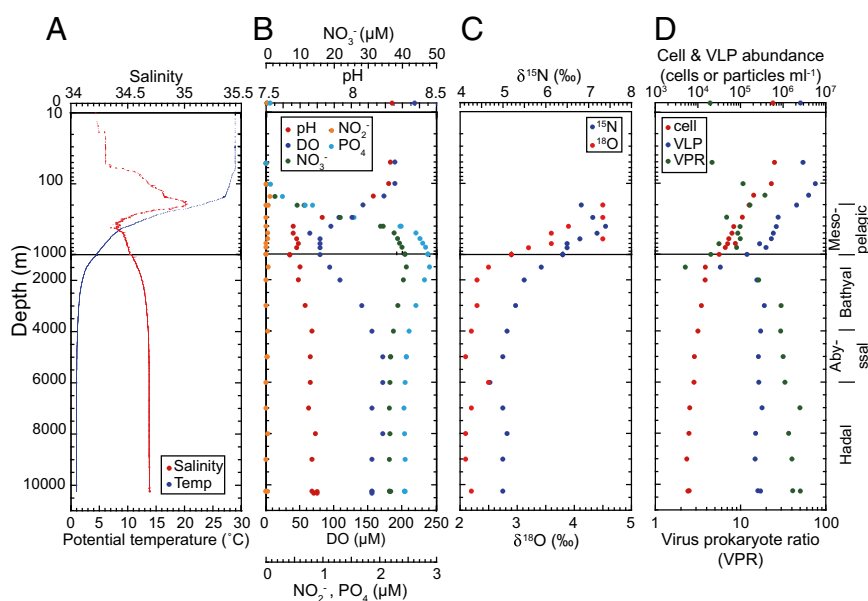
Fig. 1. Temperature and salinity (A); oxygen, nitrate, nitrite, and phosphate concentrations and pH (B); the $\delta^{15}N$ and $\delta^{18}O$ of nitrate (C); and the abundance of prokaryotic cells and VLPs and VPR (D) along the water column in the Challenger Deep. The CTD profile of temperature and salinity was obtained in dive AB#11. Other profiles were obtained by a total of three dives at the same location.
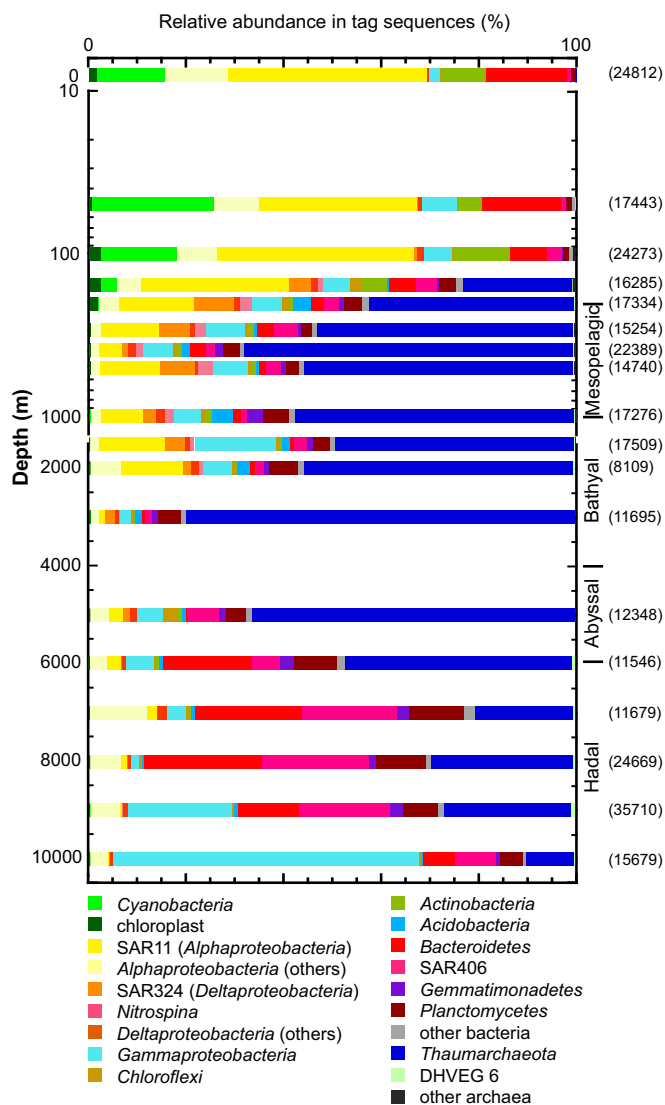
Fig. 2. Prokaryotic SSU rRNA gene community composition along the water column in the Challenger Deep. Numbers in parentheses indicate the number of tag sequences.

predominant populations above 5000 mbs. In contrast, the potential heterotrophic SAR406 (Marine Group A) and *Bacteroidetes* (10, 25) dominated the prokaryotic SSU rRNA gene communities below 6,000 mbs, whereas they were found as only a minor population above 5,000 mbs. Intriguingly, the predominance of the tag sequences closely related to *Halomonas* sp. and *Pseudomonas stutzeri* occurred at the bottom of the trench waters (9,000 and 10,241 mbs) (Fig. 2 and Dataset S2).

Among the potential nitrifier populations in the SSU rRNA gene analyses, we found niche separation for both nitrite and ammonia oxidizers along the water column. A relatively high abundance of the nitrite-oxidizing *Nitrospina* was detected in waters between 147 and 2,000 mbs, whereas the abundance of *Nitrospira* increased in the trench waters (Fig. 2 and Dataset S2). Among the potential ammonia oxidizers, the niche separation of thaumarchaeal subgroups was found along the water column, and the *Nitrosomonas* population was detected only in the trench waters. Subgroup β of the marine group I (MGI) thaumarchaeote dominated the thaumarchaeal population at the bottom of the photic zone (147–300 mbs), the δ subgroup was detected above 2,000 mbs, the α subgroup dominated the thaumarchaeal

population in the trench waters below 6,000 mbs, and the γ subgroup was detected throughout the water column below 147 mbs (Figs. S3 and S4*A*).

Detection and Quantification of Nitrifiers. To clarify the niche separation of ammonia oxidizers suggested by the SSU rRNA gene-sequencing analyses, a clone sequencing analysis was conducted for the archaeal ammonia monooxygenase α subunit (*amoA*) gene, and subsequent quantitative PCR analyses were applied for other bacterial nitrifiers to characterize the niche separation of nitrifiers in further detail. For the preparation of sufficient template DNA, amplified environmental DNA was used for the analyses. In fact, the composition of environmental DNA must be biased during the genome amplification; however, the technique has advantages in environmental molecular studies using insufficient amounts of DNA (26, 27). The archaeal *amoA* gene clone analysis suggested the distinctive distribution of four major *amoA* subgroups (A, Ba, Bb, and D) along the water column (Figs. S4*B* and S5). The niche separation of ammonia-oxidizing archaea (AOA) above the abyssal waters that suggested by the *amoA* gene clone analysis resembles the previously observed pattern that showed the distinctive distribution of the "high ammonia cluster" (HAC) and "low ammonia cluster" (LAC) of archaeal *amoA* along the water column (28) (Fig. S5). The HAC was comprised of the groups A, C, and D, and the LAC was identical to groups Ba and Bb in this study.

Based on the *amoA* sequences obtained in this study, group-specific primers for quantification were constructed for each dominant *amoA* group to clarify the niche separation of the AOA along the water column at this site. The distribution and abundance patterns obtained in the quantitative PCR were more similar to the MGI SSU rRNA gene communities than that in the archaeal *amoA* gene clone analysis (Fig. 4 and Fig. S4). Group A and Bb of *amoA* dominated in the photic zone above 200 mbs and in the mesopelagic waters above 1,000 mbs, respectively; however, *amoA* group Ba was found below 300 mbs and predominated between the mesopelagic and bathypelagic zone (300–6,000 mbs). Group D predominantly occurred in the hadal waters. The sum of the archaeal *amoA* copy number below 147 mbs correlated with archaeal SSU rRNA gene copy number below 147 mbs in the ratio of 0.9 ($R = 0.91$). The archaeal SSU rRNA gene communities below 147 mbs are dominated by the MGI thaumarchaeotes (Fig. 2), and the genomes of the MGI thaumarchaeotes in the publically accessible database are known to encode only one copy of the *amoA* and SSU rRNA genes. Thus, most of the MGI thaumarchaeotes distributed in the water column would harbor *amoA*, as suggested by Sintes et al. (28). These results also suggest the coordination between the thaumarchaeal SSU rRNA and *amoA* gene clusters: group α in the SSU rRNA gene and D in *amoA*, β and A, γ and Ba, and δ and Ba, respectively.

In addition, conventional and quantitative PCR were examined for genes from gamma- and betaproteobacterial ammonia oxidizers and nitrite-oxidizing *Nitrospira*, *Nitrospina*, and *alpha*- and *gammaproteobacteria*. The gammaproteobacterial ammonia oxidizers and alpha- and gammaproteobacterial nitrite oxidizers (e.g., *Nitrobacter* and *Nitrococcus*, respectively) were not detected throughout the water column. The betaproteobacterial *amoA* genes were revealed to be abundant in the *amoA* composition of the photic zone and the trench bottom waters, but they were absent in most depths of the mesopelagic to abyssal waters (between 400 and 5,000 mbs). Among the nitrite oxidizers, niche separation between *Nitrospina* and *Nitrospira* was also revealed. The *Nitrospira* SSU rRNA gene population outcompeted the *Nitrospina* SSU rRNA gene population in waters at 50 and 100 mbs, as well as in the hadal waters. The *Nitrospina* SSU rRNA gene abundance was higher than that of the *Nitrospira*
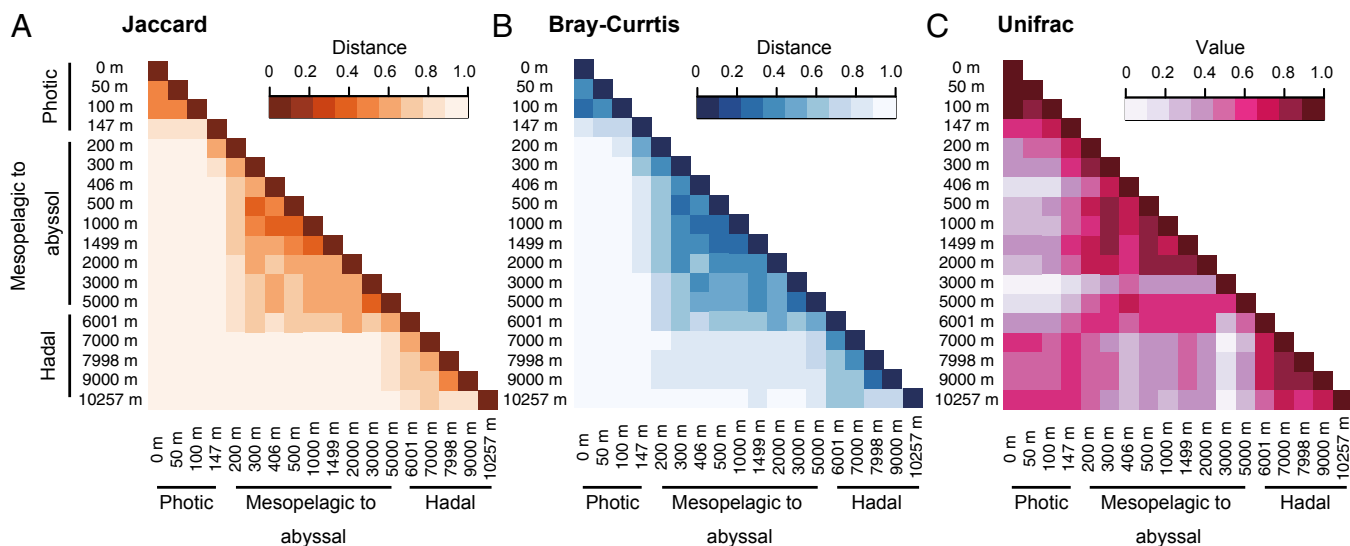
Fig. 3. Similarity matrixes of Jaccard (*A*), Bray–Curtis (*B*), and UniFrac (*C*) of the SSU rRNA gene-tag sequences.

population below the bottom of the euphotic zone to the bathyal waters (150–5,000 mbs) (Fig. 4). Gammaproteobacterial *nxrA* was not detected in this study.

Dilution Counting of Heterotrophic Bacteria. The culturable heterotrophic microbial population was estimated on board by using serial dilution cultivation of heterotrophic bacteria at 4 °C; the partial SSU rRNA gene sequences of the strains obtained from the most diluted inocula with microbial growth were determined. Surprisingly, a quite high culturable population was found (at > 2 × 10^3 cells/mL) in the trench bottom waters from 9,003 and 10,243 m, whereas the microbial cell abundances at these depths were only 5.5 and 6.3 × 10^3 cells/mL, respectively (Dataset S1). The predominant culturable heterotrophic microbes at these depths were very similar to *P. stutzeri* (99% similarity), which was consistent with the environmental SSU rRNA gene analyses at these depths (Fig. 2 and Dataset S2). Conversely, the culturable population in the upper waters (0–1,500 mbs) ranged from > 0–2 × 10^3 cells/mL and the population in deep waters (2,000–8,000 mbs) ranged from > 0 × 10 cells/mL.

Discussion

Niche Separation of Nitrifiers. The composition of nitrifiers could be indexes of carbon and nitrogen cycles in oceanic ecosystem because NH_4^+ is provided by nitrogenous organic matter decomposition. In addition, it has been noted that the niche separation of nitrifiers is regulated by the amount of available electron donors such as ammonia and nitrite (28–30). Thus, the niche separation of nitrifiers could be a signature of NH_4^+ flux from organic matter decomposition that cannot be identified from NH_4^+ concentration measurements. In fact, the SSU rRNA gene-sequencing analyses and quantitative PCR analyses of nitrifiers suggested the possible niche separation along with the transition of the entire microbial community structure and NH_4^+ flux.

Sunlight, pH, and salinity are additional significant factors that affect the niche separation of ammonia oxidizers besides the NH_4^+ concentration (31–33). The salinity change is less than 1 in the water column on the Challenger Deep and is negligible in this case. The higher abundance of ammonia-oxidizing bacteria (AOB) than AOA in the upper euphotic zone (above 50 mbs) is likely consistent with the high sensitivity of AOA to photoinhibition than the sensitivity of AOB shown by the previous cultivation experiments (31). The predominance of group A *amoA* (possibly group β MGI) in the bottom of the euphotic

zone may be associated with the relatively higher pH zone along the water column (Figs. 1*A* and 4). The co-occurrence of AOB and archaeal *amoA* group D HAC) in hadal water and the predominance of archaeal *amoA* groups Ba and Bb (LAC) in abyssal water are consistent with the previous observation that AOA prefers lower ammonia concentrations than AOB (30).

The distinctive distribution of potential nitrite oxidizers, such as the *Nitrospina* and *Nitrospira* SSU rRNA genes, was also revealed. The *Nitrospira* SSU rRNA gene population overtook the *Nitrospina* SSU rRNA gene population in waters at 50 and 100 mbs, as well as the hadal waters. The *Nitrospina* SSU rRNA gene population overcame that of the *Nitrospira* population below the bottom of the euphotic zone to the bathyal waters (150–5,000 mbs) (Fig. 4). This distribution pattern is generally consistent with the abundance of the *Nitrospina* and *Nitrospira* populations in the SSU rRNA gene-tag sequences. The significance of *Nitrospina* in the bottom of the euphotic zone to mesopelagic water is in accordance with the previous reports for (sub)tropical oceans (34–36). In contrast, the significance of *Nitrospira* in oceanic waters has not yet been revealed, although their contribution in nitrification was reported in seafloor environments (37–39). These observations could be interpreted as a result of kinetic-dependent niche separation, but several uncertainties cannot be ruled out (e.g., technical difficulties in the detection of nitrite oxidizers) (39). In general, *Nitrospira* and *Nitrospina* have typically been found in eutrophic and oligotrophic marine environments, respectively. Thus, *Nitrospira* likely adapts to a higher nitrite flux than *Nitrospina*.

Factors Controlling the Hadal Biosphere. The distribution and abundance patterns of the entire microbial and nitrifiers communities in the hadal waters were found to be distinct from those in abyssal waters. In the hadal water, the potential chemolithoautotrophs decreased in relative abundance with increasing depth and were likely replaced by the heterotrophic populations. In addition, most likely responding to the potentially elevated ammonia supply by the heterotrophic activity with increasing depth, the dominant groups of both ammonia and nitrite oxidizers were different. These results suggest that the formation of a unique hadal biosphere in the Challenger Deep may be driven by the input of organic matter and the following heterotrophic degradation; however, the distribution and abundance patterns of microbial communities cannot be explained by the vertical flux of sinking organic particles.
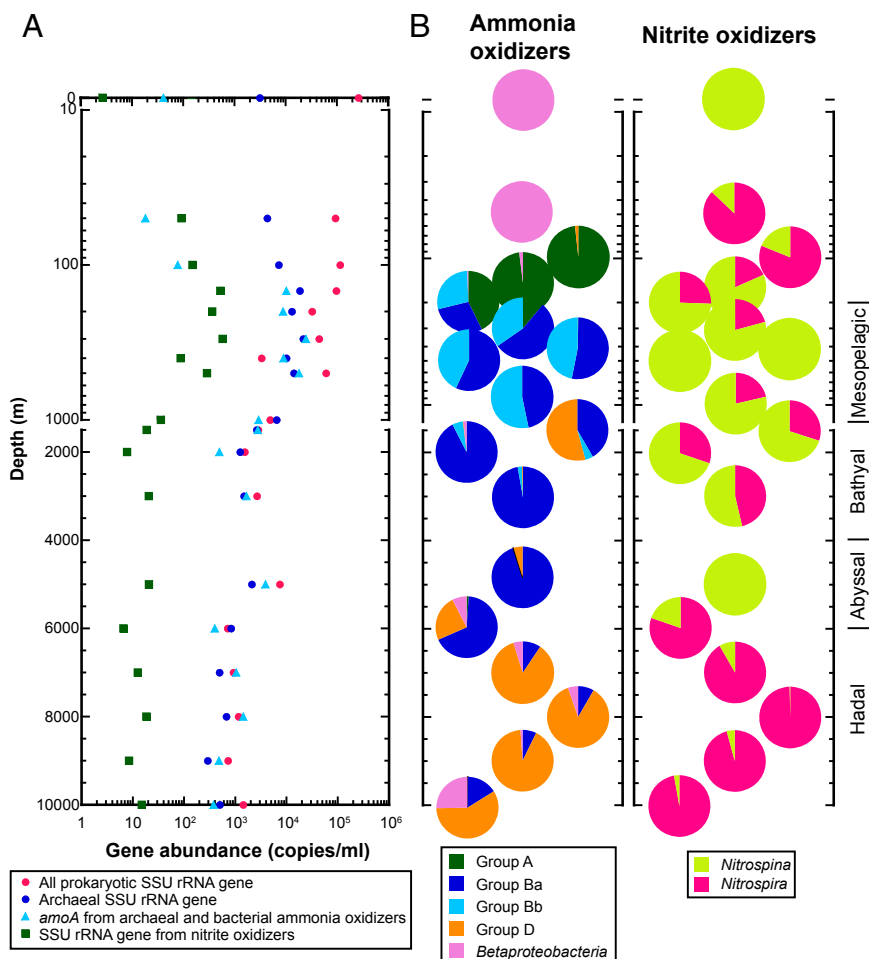
Fig. 4. The abundance of whole prokaryotic, archaeal and nitrite oxidizer SSU rRNA and *amoA* genes (*A*), and the abundance of subgroups of *amoA* genes and SSU rRNA genes of nitrite-oxidizing bacteria (*B*) along the water column in the Challenger Deep obtained by quantitative PCR. Grouping of *amoA* are shown in Fig. S5.

The Challenger Deep is located in the oligotrophic ocean region and is geographically and hydrotopographically isolated from other trenches in the Western Pacific. Thus, endogenous organic carbon sources are required to support the hadal water heterotrophic microbial communities. Recent studies have pointed to the importance of suspended organic matter, including both sinking and suspended organic matter in bathypelagic waters (40, 41). In addition, Kawagucci et al. reported the impacts of suspended sediment associated with huge earthquakes that affected the microbial communities in the bathyal and abyssal water ecosystems (42). The microbial heterotrophic populations influenced by the suspended organic matter were similar to those found in the Challenger Deep hadal biosphere that were enriched by heterotrophs. A steep slope, narrow geomorphology, slow trench current (8, 9), and earthquakes may supply a steady state or the occasional input of sinking and suspended organic matter. Because suspended particulate matters are transported vertically as well as horizontally (42, 43), the suspended organic matter from slopes likely influences the geochemical cycle in the entire trench waters. The higher sediment deposition rate in the trench bottom compared with the adjacent abyssal plain (13), as well as the clear stratification of trench bottom sediment under the sampling site (Fig. S6), also suggest the occasional input of sediment supply from the trench slope. Moreover, the slightly elevated salinity of the bottom water could induce the density-driven stratification of

hadal water mass (9). The stratification of hadal water mass may promote the development of isolated and unique biogeochemical cycles and microbial communities. This study hypothesizes that the unique microbial ecosystem in one of the deepest accessible biospheres on this planet is primarily driven by the geomorphology of the Mariana Trench.

Experimental Procedures

Site Description and Sampling. A total of three dives for the ROV *ABISMO* was conducted in the Challenger Deep of the Mariana Trench (11°22.25′N, 142°42.75′E, 10,300 m) during the Japan Agency for Marine-Earth Science & Technology (JAMSTEC) *R/V Kairei* KR08-05 cruise (June 2008) (44) (Dataset S1). Temperature, depth, and salinity were measured using a conductivity, temperature, and depth (CTD) sensor SBE49 (Sea-Bird Electronics). Waters from near the bottom of the trench (water depth of approx. 10,300 m) to the surface were taken using Niskin bottles (5 L) (General Oceanic) that were settled on the ROV *ABISMO*. Sea-surface water was collected using a bucket. The water samples used in this study are summarized in Dataset S1, and the sub-samples for geochemical and microbiological analyses were taken from the same bottles. Samples for cell counting were fixed by formaldehyde [final concentration 3% (vol/vol)], and filtered on a polycarbonate membrane filter (0.2 μm). The filters were stored at –80 °C. The water samples for counting virus-like particles were filtered with cellulose nitrate membrane filter (0.2 μm), fixed by formaldehyde [final concentration 3% (vol/vol)], frozen in liquid nitrogen, and then stored at –80 °C. Microbial cells in each 2–3 L water for molecular ecological analyses were collected on cellulose nitrate membrane filters, and stored at –80 °C. Trench bottom sediment was obtained by a gravity corer of the ROV *ABISMO* in the same dive. A sediment core was split onboard and stored at 5 °C.

Geochemical Analyses. DO was measured using an oxygen CHEMets kit (CHEMeytrics) onboard. Samples for nutrient analysis were filtrated with 0.2-μm cellulose acetate filter and stored at −20 °C until further analysis. Concentrations of NO_3^-, NO_2^-, PO_4^-, and NH_4^+ were analyzed spectrophotometrically using an automated QuAAtro 2-HR analyzer (BL TEC).

Nitrogen and oxygen isotopic compositions of the nitrate were determined using the denitrifier method (45–47). Nitrate was converted to N_2O by the strain *Pseudomonas chlororaphis* (JCM20509 = ATCC13985), a denitrifying bacterium lacking the capability of N_2O reduction (46). Then, the produced nitrous oxide was extracted, purified, and measured for nitrogen and oxygen isotopic ratios using a 20–22 continuous flow isotope ratio mass spectrometer (Sercon) at Tokyo University of Agriculture and Technology. The amount of nitrous oxide introduced to CF-IRMS ranged from 3 to 15 nmol. International isotopic reference materials, USGS32 ($\delta^{15}N = 180‰$, $\delta^{18}O = 25.7‰$), USGS34 ($\delta^{15}N = −1.8‰$, $\delta^{18}O = -27.9‰$), USGS35 ($\delta^{18}O = 57.5‰$) and IAEA-NO_3 ($\delta^{15}N = 4.7‰$, $\delta^{18}O = 25.6‰$) (47–49), were used for the calibration. The $\delta^{15}N$ values were reported relative to atmospheric N_2, and the $\delta^{18}O$ values were reported relative to standard mean ocean water (V-SMOW). The analytical precision of in-house material was typically less than 0.2‰ for $\delta^{15}N$ and 0.3‰ for $\delta^{18}O$.

DNA Extraction and Amplification. Environmental DNA was extracted from the cells on cellulose nitrate membrane filters using a Soil DNA Isolation Kit (Mo-Bio Lab) with minor modifications. A portion of environmental DNA was amplified using a REPLI-g Mini Kit (Qiagen) for the molecular analyses described below. Amplified DNA assemblages were digested by S1 nuclease (Invitrogen) before the following studies.

Diversity Analyses for SSU rRNA and Archaeal *amoA* Genes. Prokaryotic SSU rRNA gene fragments were amplified with a primer set of 530F and 907R (50) from the original environmental DNA assemblages using LA Taq polymerase with GC buffer (Takara Bio) as previously described (50). For tag sequencing, primers with 10 bp of extended tag sequences in 5′-termini were used for the SSU rRNA gene amplification. For archaeal *amoA* clone analysis, gene fragments were obtained using EX Taq polymerase (Takara Bio) from the amplified environmental DNA assemblages. The amplification conditions and primer sequences for each of the PCR amplifications are summarized in Table S1.

For the clone analyses, amplified DNA fragments were cloned into pCR2.1 vector (Invitrogen), and clone libraries were constructed. The inserts were directly sequenced with the M13M4 primer using an ABI3730xl genetic analyzer with Big Dye v3.1. SSU rRNA gene sequences with >97% identity were assigned as the same clone type (phylotype) based on FastGroup II (51) and similarity analysis in GENETYX-MAC v15 (GENETYX). SSU rRNA gene amplicons for tag sequencing were analyzed by 454 FLX Titanium sequencer (Roche). All of the raw tag sequences were treated with shhh.flows pipeline in MOTHUR 1.31.1 (52–54), and the primer sequences in either or both ends of the tags were eliminated. Tag sequences shorter than 300 bp were removed from the downstream analyses. Potential chimera sequences were surveyed using UCHIME (55). Next, phylogenetic assignment and statistical analyses for the tag sequences were conducted. Sequencing tags were aligned using the partial order algorithm (SINA; www.arb-silva.de/aligner/) with the reference multiple alignment SILVA SSU Ref NR (56). All of the aligned sequences were then clustered into operational taxonomic units (OTUs) by 97% sequence identity using MOTHUR 1.31.1, with default parameters according to the average-clustering algorithm. Output was then parsed to produce occurrence tables of each OTU in each sample. The taxonomic position of each OTU was automatically assigned based on Blast analysis in the QIIME software package (57) using SILVA Ref NR as a reference dataset of SSU rRNA gene sequences. The sequences were excluded that are closely related to the potential contaminants belonging to genera that inhabit soil and the human body and have been detected from negative control experiments of environmental microbiology in the laboratory, such as *Bradyrhizobium*, *Brevundimonas*, *Burkholderiaceae*, *Delftia*, *Erythrobacter*, *Lactococcus*, *Legionella*, *Methylobacterium*, *Mycobacterium*, *Neisseria*, *Novosphingobium*, *Propionibacterium*, *Sphingobium*, *Sphingomonas*, *Sphingopyxis*, *Staphylococcus*, *Stenotrophomonas*, and *Streptococcus*. Sequences presenting with relatively high E-values (>1.0E-30) or low identity (<90%) to the best match sequence were designated as other archaea or bacteria, and sequences that did not present significant similarity to any reference sequences were also excluded from the analysis. α-Diversity indices (rarefaction curves, Chao1, ACE, Shannon, Shannon evenness, and Simpson) in each library and taxa/divisions were also calculated using MOTHUR 3.6. The

Jaccard and Bray–Curtis dissimilarity indices among each library were estimated using the vegan package in the R-environment (vegan.r-forge.r-project.org). Phylogenetic trees were constructed from the curated alignment of representative sequences using the Clustal W program (www.clustal.org). A weighted UniFrac distance matrix among core samples was constructed from the phylogenetic tree and a sample mapping files that showed frequency of the sequence tags within OTUs. Sequencing tags for each phylum/class were collected from the entire dataset in accordance with the taxonomic position of each OTU in the case of the entire dataset. The subdatasets were analyzed as in the case of the entire dataset.

All SSU rRNA gene sequences obtained in this study were compared using the UniFrac program (58) after omitting potential chimera sequences and potential experimental contamination sequences. The alignment of each SSU rRNA gene clone library was constructed using the SINA alignment service (www.arb-silva.de/aligner/) (59). The phylogenetic tree of all SSU rRNA gene sequence obtained in this study was constructed by Clustal X (www.clustal.org), and the principal component analysis was carried out using the tree by UniFrac. Representative SSU rRNA gene sequences were aligned and phylogenetically classified into certain taxonomic units using ARB (56). The phylogenetic tree of thaumarchaeal SSU rRNA genes was constructed by Clustal X based on the unambiguous residues. Representative *amoA* sequences were automatically aligned with closely related nucleotide sequences, and the phylogenetic tree was then constructed using Clustal X v2.0 (60).

Quantitative PCR Analyses. Primers, probes and components of standard mixture used for the quantitative PCR analyses are summarized in Table S1. The abundance of each gene was quantified as an average of the duplicate or triplicate analyses. Original DNA assemblages were only used for the quantification of archaeal and prokaryotic SSU rRNA genes, and the amplified DNA assemblages were used for the other genes. The abundance of nitrifier genes in each water mass was estimated from the relative abundance of archaeal SSU rRNA gene and a respective gene in the amplified DNA assemblages.

The 7500 Real Time PCR System (Applied Biosystems) was used for all of the quantitative PCR analyses in this study. Quantification of the archaeal and all prokaryotic SSU rRNA genes was performed using both the original and amplified environmental DNA (Table S1). Detection and quantification of nitrifiers were assessed using the amplified environmental DNA assemblages. Detection of the alpha- and betaproteobacterial *nxrA* and alphaproteobacterial *amoA* was examined using Ex Taq polymerase (Takara Bio) with a Mg^{2+} buffer as described previously (39) (Table S1). The abundance of *Nitrospina* and *Nitrospira* SSU rRNA genes was also examined according to methods described previously (39, 61). To identify group specific distribution of each archaeal *amoA* group, novel primer sets were constructed based on archaeal *amoA* gene sequences obtained in this study as follows: The nucleotide alignments of the archaeal *amoA* gene were constructed by Clustal X v2.0, and primers were designed that individually matched with the specific *amoA* sequences in groups A, Ba, Bb, and D (Table S1).

For the preparation of quantitative PCR mixtures, qPCR Quick GoldStar Mastermix Plus (Eurogentec) was applied for SSU rRNA genes of archaea, all prokaryotes and *Nitrospira*, and a SYBR Premix Ex Taq II (Takara Bio) for *amoA* genes and the *Nitrospina* SSU rRNA gene. Amplified products from quantitative PCR using SYBR Premix reagent were confirmed by agarose gel electrophoresis. Amplification specificity was confirmed by clone analysis for amplicons from several depths, particularly in the cases of *amoA* genes.

Dilution Counting for Heterotrophs. The abundance of culturable heterotrophs at each depth was evaluated onboard by serial dilution cultivation methods with 1×, 1/100×, and 1/10,000× Marine Broth (Difco) using 96-well microtiter plates at 5 °C for 2 mo under atmospheric pressure. For the dilution of Marine Broth, MJ synthetic seawater (62) was used. Then, SSU rRNA gene sequences from the cultures obtained from the most diluted wells were amplified with a primer set of B27F and U1492R (Table S1), and directly sequenced using the ABI3730xl genetic analyzer with Big Dye v3.1 (Applied Biosystems) according to the manufacturer's recommendations.

1. Guidi L, et al. (2009) Effects of phytoplankton community on production, size and export of large aggregates: A world-ocean analysis. *Limnol Oceanogr* 54(6):1951–1963.

2. Bochdansky AB, van Aken HM, Herndl GJ (2010) Role of macroscopic particles in deep-sea oxygen consumption. *Proc Natl Acad Sci USA* 107(18):8287–8291.

3. Herndl GJ, Reinthaler T (2013) Microbial control of the dark end of the biological pump. *Nat Geosci* 6(9):718–724.

4. Yokokawa T, Yang Y, Motegi C, Nagata T (2013) Large-scale geographical variation in prokaryotic abundance and production in meso-and bathypelagic zones of the central Pacific and Southern Ocean. *Limnol Oceanogr* 58(1):61–73.

5. Alonso-Sáez L, Galand PE, Casamayor EO, Pedrós-Alió C, Bertilsson S (2010) High bicarbonate assimilation in the dark by Arctic bacteria. *ISME J* 4(12):1581–1590.

6. Swan BK, et al. (2011) Potential for chemolithoautotrophy among ubiquitous bacteria lineages in the dark ocean. *Science* 333(6047):1296–1300.

7. Jamieson AJ, Fujii T, Mayor DJ, Solan M, Priede IG (2010) Hadal trenches: The ecology of the deepest places on Earth. *Trends Ecol Evol* 25(3):190–197.

8. Taira K, Kitagawa S, Yamashiro T, Yanagimoto D (2004) Deep and bottom currents in the challenger deep, measured with super-deep current meters. *J Oceanogr* 60(6):919–926.

9. Taira K, Yanagimoto D, Kitagawa S (2005) Deep CTD casts in the Challenger Deep, Mariana Trench. *J Oceanogr* 61(3):447–454.

10. Nagata T, et al. (2010) Emerging concepts on microbial processes in the bathypelagic ocean—Ecology, biogeochemistry, and genomics. *Deep Sea Res Part II Top Stud Oceanogr* 57(16):1519–1536.

11. Bartlett DH (2009) Microbial life in the trenches. *MTS J* 43(5):128–131.

12. Tamburini C, Boutrif M, Garel M, Colwell RR, Deming JW (2013) Prokaryotic responses to hydrostatic pressure in the ocean—A review. *Environ Microbiol* 15(5):1262–1274.

13. Glud RN, et al. (2013) High rates of microbial carbon turnover in sediments in the deepest oceanic trench on Earth. *Nat Geosci* 6(4):284–288.

14. Takami H, Inoue A, Fuji F, Horikoshi K (1997) Microbial flora in the deepest sea mud of the Mariana Trench. *FEMS Microbiol Lett* 152(2):279–285.

15. Kato C, et al. (1998) Extremely barophilic bacteria isolated from the Mariana Trench, Challenger Deep, at a depth of 11,000 meters. *Appl Environ Microbiol* 64(4):1510–1513.

16. Fujioka K, Okino K, Kanamatsu T, Ohara Y (2002) Morphology and origin of the Challenger Deep in the Southern Mariana Trench. *Geophy Res Let* 29(10):10-1–10-4.

17. Yoshida M, Takaki Y, Eitoku M, Nunoura T, Takai K (2013) Metagenomic analysis of viral communities in (hado)pelagic sediments. *PLoS ONE* 8(2):e57271.

18. Mantyla AW, Reid JL (1978) Measurements of water characteristics at depths greater than 10 km in the Marianas Trench. *Deep-Sea Res* 25(2):169–173.

19. Sigman DM, et al. (2009) The dual isotopes of deep nitrate as a constraint on the cycle and budget of oceanic fixed nitrogen. *Deep Sea Res Part I Oceanogr Res Pap* 56(9):1419–1439.

20. Giovannoni SJ, et al. (2005) Proteorhodopsin in the ubiquitous marine bacterium SAR11. *Nature* 438(7064):82–85.

21. Gómez-Consarnau L, et al. (2007) Light stimulates growth of proteorhodopsin-containing marine *Flavobacteria*. *Nature* 445(7124):210–213.

22. Ghai R, Mizuno CM, Picazo A, Camacho A, Rodriguez-Valera F (2013) Metagenomics uncovers a new group of low GC and ultra-small marine *Actinobacteria*. *Sci Rep* 3:2471.

23. Chitsaz H, et al. (2011) Efficient de novo assembly of single-cell bacterial genomes from short-read data sets. *Nat Biotechnol* 29(10):915–921.

24. Sheik CS, Jain S, Dick GJ (2014) Metabolic flexibility of enigmatic SAR324 revealed through metagenomics and metatranscriptomics. *Environ Microbiol* 16(1):304–317.

25. Wright JJ, et al. (2014) Genomic properties of Marine Group A bacteria indicate a role in the marine sulfur cycle. *ISME J* 8(2):455–468.

26. Chen Y, et al. (2008) Revealing the uncultivated majority: Combining DNA stable-isotope probing, multiple displacement amplification and metagenomic analyses of uncultivated *Methylocystis* in acidic peatlands. *Environ Microbiol* 10(10):2609–2622.

27. Bodelier PLE, Kamst M, Meima-Franke M, Stralis-Pavese N, Bodrossy L (2009) Whole-community genome amplification (WCGA) leads to compositional bias in methane-oxidizing communities as assessed by *pmoA*-based microarray analyses and QPCR. *Environ Microbiol Rep* 1(5):434–441.

28. Sintes E, Bergauer K, De Corte D, Yokokawa T, Herndl GJ (2013) Archaeal *amoA* gene diversity points to distinct biogeography of ammonia-oxidizing *Crenarchaeota* in the ocean. *Environ Microbiol* 15(5):1647–1658.

29. Blackburne R, Vadivelu VM, Yuan Z, Keller J (2007) Kinetic characterisation of an enriched Nitrospira culture with comparison to *Nitrobacter*. *Water Res* 41(14):3033–3042.

30. Martens-Habbena W, Berube PM, Urakawa H, de la Torre JR, Stahl DA (2009) Ammonia oxidation kinetics determine niche separation of nitrifying *Archaea* and *Bacteria*. *Nature* 461(7266):976–979.

31. Merbt SN, et al. (2012) Differential photoinhibition of bacterial and archaeal ammonia oxidation. *FEMS Microbiol Lett* 327(1):41–46.

32. Gubry-Rangin C, et al. (2011) Niche specialization of terrestrial archaeal ammonia oxidizers. *Proc Natl Acad Sci USA* 108(52):21206–21211.

33. Mosier AC, Francis CA (2008) Relative abundance and diversity of ammonia-oxidizing archaea and bacteria in the San Francisco Bay estuary. *Environ Microbiol* 10(11):3002–3016.

34. Mincer TJ, et al. (2007) Quantitative distribution of presumptive archaeal and bacterial nitrifiers in Monterey Bay and the North Pacific Subtropical Gyre. *Environ Microbiol* 9(5):1162–1175.

35. Santoro AE, Casciotti KL, Francis CA (2010) Activity, abundance and diversity of nitrifying archaea and bacteria in the central California Current. *Environ Microbiol* 12(7):1989–2006.

36. Füssel J, et al. (2012) Nitrite oxidation in the Namibian oxygen minimum zone. *ISME J* 6(6):1200–1209.

37. Hoffmann F, et al. (2009) Complex nitrogen cycling in the sponge *Geodia barretti*. *Environ Microbiol* 11:2228–2243.

38. Off S, Alawi M, Spieck E (2010) Enrichment and physiological characterization of a novel *Nitrospira*-like bacterium obtained from a marine sponge. *Appl Environ Microbiol* 76(14):4640–4646.

39. Nunoura T, et al. (2013) Molecular biological and isotopic biogeochemical prognoses of the nitrification-driven dynamic microbial nitrogen cycle in hadopelagic sediments. *Environ Microbiol* 15(11):3087–3107.

40. Baltar F, et al. (2009) Evidence of prokaryotic metabolism on suspended particulate organic matter in the dark waters of the subtropical North Atlantic. *Limnol Oceanogr* 54(1):182–193.

41. Aristegui J, Gasol JM, Duarte CM, Herndl GJ (2009) Microbial oceanography of the dark ocean's pelagic realm. *Limnol Oceanogr* 54(5):1501–1529.

42. Kawagucci S, et al. (2012) Disturbance of deep-sea environments induced by the M9.0 Tohoku Earthquake. *Sci Rep* 2:270.

43. Otosaka S, Noriki S (2000) REEs and Mn/Al ratio of settling particles: Horizontal transport of particulate material in the northern Japan Trench. *Mar Chem* 72(2-4):329–342.

44. Yoshida H, et al. (2009) The *ABISMO* mud and water sampling ROV for surveys at 11,000 m depth. *MTS J* 43(5):87–96.

45. Sigman DM, et al. (2001) A bacterial method for the nitrogen isotopic analysis of nitrate in seawater and freshwater. *Anal Chem* 73(17):4145–4153.

46. Casciotti KL, Sigman DM, Hastings MG, Böhlke JK, Hilkert A (2002) Measurement of the oxygen isotopic composition of nitrate in seawater and freshwater using the denitrifier method. *Anal Chem* 74(19):4905–4912.

47. McIlvin MR, Casciotti KL (2011) Technical updates to the bacterial method for nitrate isotopic analyses. *Anal Chem* 83(5):1850–1856.

48. Böhlke JK, Coplen TB (1995) *Reference and Intercomparison Materials for Stable Isotopes of Light Elements. IAEA TECDOC 825* (International Atomic Energy Agency, Vienna), pp 51–66.

49. Böhlke JK, Mroczkowski SJ, Coplen TB (2003) Oxygen isotopes in nitrate: New reference materials for ^{18}O:^{17}O:^{16}O measurements and observations on nitrate-water equilibration. *Rapid Commun Mass Spectrom* 17(16):1835–1846.

50. Nunoura T, et al. (2012) Microbial diversity in deep-sea methane seep sediments presented by SSU rRNA gene tag sequencing. *Microbes Environ* 27(4):382–390.

51. Yu Y, Breitbart M, McNairnie P, Rohwer F (2006) FastGroupII: A web-based bioinformatics platform for analyses of large 16S rDNA libraries. *BMC Bioinformatics* 7:57.

52. Quince C, et al. (2009) Accurate determination of microbial diversity from 454 pyrosequencing data. *Nat Methods* 6(9):639–641.

53. Schloss PD, et al. (2009) Introducing MOTHUR: Open-source, platform-independent, community-supported software for describing and comparing microbial communities. *Appl Environ Microbiol* 75(23):7537–7541.

54. Schloss PD, Gevers D, Westcott SL (2011) Reducing the effects of PCR amplification and sequencing artifacts on 16S rRNA-based studies. *PLoS ONE* 6(12):e27310.

55. Edgar RC, Haas BJ, Clemente JC, Quince C, Knight R (2011) UCHIME improves sensitivity and speed of chimera detection. *Bioinformatics* 27(16):2194–2200.

56. Yilmaz P, et al. (2014) The SILVA and "All-species Living Tree Project (LTP)" taxonomic frameworks. *Nucleic Acids Res* 42(Database issue, D1):D643–D648.

57. Caporaso JG, et al. (2010) QIIME allows analysis of high-throughput community sequencing data. *Nat Methods* 7(5):335–336.

58. Lozupone C, Hamady M, Knight R (2006) UniFrac—An online tool for comparing microbial community diversity in a phylogenetic context. *BMC Bioinformatics* 7(1):371.

59. Pruesse E, Peplies J, Glöckner FO (2012) SINA: Accurate high-throughput multiple sequence alignment of ribosomal RNA genes. *Bioinformatics* 28(14):1823–1829.

60. Larkin MA, et al. (2007) Clustal W and Clustal X version 2.0. *Bioinformatics* 23(21):2947–2948.

61. Graham DW, et al. (2007) Experimental demonstration of chaotic instability in biological nitrification. *ISME J* 1(5):385–393.

62. Sako Y, Takai K, Ishida Y, Uchida A, Katayama Y (1996) *Rhodothermus obamensis* sp. nov., a modern lineage of extremely thermophilic marine bacteria. *Int J Syst Bacteriol* 46(4):1099–1104.